Diffraction at TOTEM

G. Antchev[1], *P. Aspell*[1], *V. Avati*[1,9], *M.G. Bagliesi*[5], *V. Berardi*[4], *M. Berretti*[5], *M. Besta*[1], *M. Bozzo*[2], *E. Brücken*[6], *A. Buzzo*[2], *F. Cafagna*[4], *M. Calicchio*[4], *M.G. Catanesi*[4], *R. Cecchi*[5], *M.A. Ciocci*[5], *P. Dadel*[1], *M. Deile*[1], *E. Dimovasili*[1,9], *K. Eggert*[9], *V. Eremin*[11], *F. Ferro*[2], *A. Fiergolski*[1], *F. Garcia*[6], *S. Giani*[1]*, *V. Greco*[5], *L. Grzanka*[1], *J. Heino*[6], *T. Hildén*[6], *J. Kašpar*[1,7], *J. Kopal*[1,7], *V. Kundrát*[7], *K. Kurvinen*[6], *S. Lami*[5], *G. Latino*[5], *R. Lauhakangas*[6], *R. Leszko*[1], *E. Lippmaa*[8], *M. Lokajíček*[7], *M. Lo Vetere*[2], *F. Lucas Rodriguez*[1], *M. Macrí*[2], *G. Magazzù*[5], *M. Meucci*[5], *S. Minutoli*[2], *H. Niewiadomski*[1,9]†, *G. Notarnicola*[4], *E. Oliveri*[5], *F. Oljemark*[6], *R. Orava*[6], *M. Oriunno*[1], *K. Österberg*[6], *E. Pedreschi*[5], *J. Petäjäjärvi*[6], *J. Prochazka*[7], *M. Quinto*[4], *E. Radermacher*[1], *E. Radicioni*[4], *F. Ravotti*[1], *G. Rella*[4], *E. Robutti*[2], *L. Ropelewski*[1], *M. Rostkowski*[1], *G. Ruggiero*[1], *A. Rummel*[8], *H. Saarikko*[6], *G. Sanguinetti*[5], *A. Santroni*[2], *A. Scribano*[5], *G. Sette*[2], *W. Snoeys*[1], *F. Spinella*[5], *A. Ster*[10], *C. Taylor*[3], *A. Trummal*[8], *N. Turini*[5], *J. Whitmore*[9], *J. Wu*[1], *M. Zalewski*[1]

[1]CERN, Genève, Switzerland,
[2]Università di Genova and Sezione INFN, Genova, Italy,
[3]Case Western Reserve University, Dept. of Physics, Cleveland, OH, USA,
[4]INFN Sezione di Bari and Politecnico di Bari, Bari, Italy,
[5]INFN Sezione di Pisa and Università di Siena, Italy,
[6]Helsinki Institute of Physics and Department of Physics, University of Helsinki, Finland,
[7]Institute of Physics of the Academy of Sciences of the Czech Republic, Praha, Czech Republic,
[8]National Institute of Chemical Physics and Biophysics NICPB, Tallinn, Estonia.
[9]Penn State University, Dept. of Physics, University Park, PA, USA.
[10]MTA KFKI RMKI, Budapest, Hungary.
[11]Ioffe Physico-Technical Institute, Polytechnicheskaya Str. 26, 194021 St-Petersburg, Russian Federation.

The primary objective of the TOTEM experiment at the LHC is the measurement of the total proton-proton cross section with the luminosity-independent method and the study of elastic proton-proton cross-section over a wide $|t|$-range. In addition TOTEM also performs a comprehensive study of diffraction, spanning from cross-section measurements of individual diffractive processes to the analysis of their event topologies. Hard diffraction will be studied in collaboration with CMS taking advantage of the large common rapidity coverage for charged and neutral particle detection and the large variety of trigger possibilities even at large luminosities. TOTEM will take data under all LHC beam conditions including standard high luminosity runs to maximise its physics reach. This contribution describes the main features of the TOTEM diffractive physics programme including measurements to be made in the early LHC runs.

* corresponding author: Simone Giani (simone.giani@cern.ch)
† corresponding author: Hubert Niewiadomski (hubert.niewiadomski@cern.ch)

1 Introduction

The TOTEM experiment [1, 2] will measure the total proton-proton cross-section with the luminosity-independent method based on the Optical Theorem, which requires a detailed study of the elastic scattering cross-section down to a squared four-momentum transfer of $|t| \sim 10^{-3}\,\mathrm{GeV}^2$ and the measurement of the total inelastic rate. Furthermore, TOTEM's physics programme aims at a deeper understanding of the proton structure by studying elastic scattering with large momentum transfers, and via the diffractive processes — partly in cooperation with CMS [3], located at the same interaction point, IP5.

To perform these measurements, TOTEM requires a good acceptance for particles produced at very small angles with respect to the beam. TOTEM's coverage in the pseudorapidity range of $3.1 \leq |\eta| \leq 6.5$ on both sides of the interaction point is accomplished by two telescopes for inelastically produced particles. This is complemented by detectors in special movable beam-pipe insertions — so-called Roman Pots — placed at 147 and 220 m from the interaction point, designed to track leading protons at a few mm from the beam centre.

For the luminosity-independent total cross-section measurement, TOTEM has to reach the lowest possible $|t|$ values in elastic pp scattering. Elastically scattered protons close to the beam can be detected downstream on either side of the IP if the displacement at the detector location is large enough and if the beam divergence at the IP is small compared to the scattering angle. To achieve these conditions special LHC optics with high beta value at the IP (β^*) is required. According to Liouville's theorem [4, 5], the larger the β^*, which determines the beam size, the smaller the beam divergence ($\sim 1/\sqrt{\beta^*}$). Two optics are proposed: an ultimate one with $\beta^* = 1535\,\mathrm{m}$ and another one, likely foreseen for 2010, with $\beta^* = 90\,\mathrm{m}$. The latter uses the standard injection optics ($\beta^* = 11\,\mathrm{m}$) and beam conditions typical for early LHC running: zero degree crossing-angle and consequently at most 156 bunches together with a low number of protons per bunch.

2 Diffraction in TOTEM

Diffractive final states will comprise almost 50 % of all final states at the LHC. Their study will shed light on the proton structure and will help in understanding the transition between the non-perturbative regime of low-t elastic scattering and that of hard diffraction, where rapidity gaps and forward protons co-exist with large $\mathbf{p}_T$ final states.

A general definition of hadronic diffractive process states that diffraction is a reaction in which no quantum numbers are exchanged between the colliding particles [6]. The traditional theoretical framework for diffraction — Regge theory — explains diffractive reactions at high energies in terms of Pomeron exchange. Many consider the concept of Pomeron misleading and thus current research aims at understanding this exchange in terms of QCD.

It is difficult to determine experimentally if the outgoing systems have the same quantum numbers as the incoming particles. Therefore, the operational definition is introduced, which classifies a process to be diffractive on the basis of the non-exponentially suppressed rapidity gap $\Delta\eta$ in the final state: $\mathrm{d}N/\mathrm{d}\Delta\eta \sim \mathrm{const}$, while the non-diffractive events are exponentially suppressed: $\mathrm{d}N/\mathrm{d}\Delta\eta \sim \mathrm{e}^{-\Delta\eta}$.

Given its unique coverage for charged particles at high rapidities, TOTEM is ideal for studies of forward phenomena. Since energy flow and particle multiplicity of inelastic events peak in the forward region, the large rapidity coverage and proton detection on both sides allow the

study of a wide range of processes in inelastic and diffractive interactions.

Diffractive scattering comprises Single Diffraction (SD), Double Diffraction (DD), Double Pomeron Exchange (DPE) (Central Diffraction), and higher order multi-Pomeron processes. Together with elastic scattering these processes represent about 50 % of the total cross-section. Many details of these processes with close ties to proton structure and low-energy QCD are still poorly understood.

Majority of diffractive events ($\sim 35\,\%$) (Figure 1) exhibit intact protons in the final state,

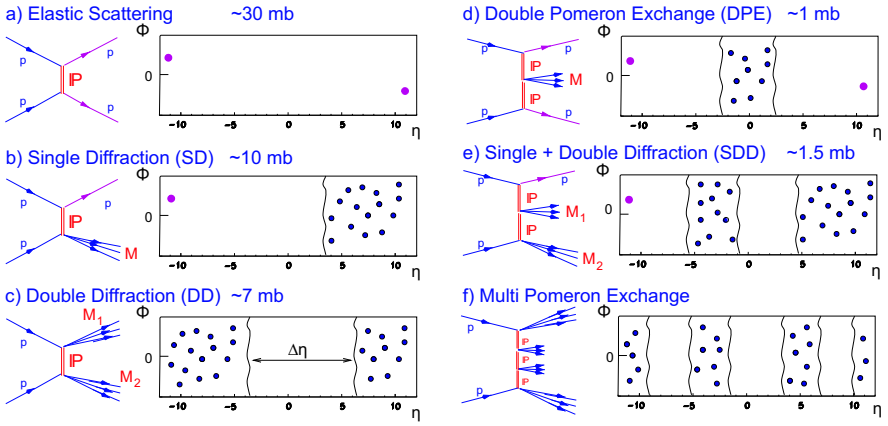

Figure 1: Different classes of diffractive processes and their cross-sections as estimated for the LHC at $\sqrt{s} = 14\,\text{TeV}$.

characterised by their t and by their ξ. For large β^* (see Figure 2, right) most of these protons can be detected in the RP detectors.

3 LHC Optics

The transport of protons in the LHC lattice can be expressed by two optical functions $L_{x,y}$ (effective length) and $v_{x,y}$ (magnification). According to the general form of the transport matrix (see [5]), their values, at a distance s from the IP, depend upon the betatron function $\beta(s)$ and the phase advance $\Delta\mu(s)$. Since $\beta(s)$ is at extremum in the IP, the functions $v(s)$ and $L(s)$ can be expressed as $v(s) = \sqrt{\frac{\beta(s)}{\beta^*}}\cos\Delta\mu(s)$ and $L(s) = \sqrt{\beta(s)\beta^*}\sin\Delta\mu(s)$ with $\Delta\mu(s) = \int_0^s \frac{1}{\beta(s')}ds'$.

The transverse displacement $(x(s), y(s))$ of a proton at a distance s from the IP is related to its transverse origin (x^*, y^*) and its momentum vector (expressed by the horizontal and vertical scattering angles Θ_x^* and Θ_y^*, and by $\xi = \Delta p/p$) at the IP via the above optical functions and the horizontal dispersion $D_x(s)$ of the machine:

$$\begin{aligned} y(s) &= v_y(s)\cdot y^* + L_y(s)\cdot\Theta_y^* \\ x(s) &= v_x(s)\cdot x^* + L_x(s)\cdot\Theta_x^* + \xi\cdot D_x(s). \end{aligned} \tag{1}$$

As a consequence of the high β^*, the beam size at the IP is large ($\sigma^*_{beam} \sim \sqrt{\beta^*}$), which reduces the luminosity for such a running scenario. To eliminate the dependence on the transverse

position of the proton at the collision point, the magnification has to be chosen close to zero (parallel-to-point focussing, $\Delta\mu = \pi/2$). At the same time, a large effective length ensures a sizeable displacement of scattered protons from the beam centre.

Having in mind the above optimisation for the position of the RP220 station, two scenarios have been studied. Their optical functions are compared in Table 1, together with standard

β^* [m]	L_x [m]	L_y [m]	v_x	v_y	D_x [m]	$x_{\rm RP}$ [mm]	$y_{\rm RP}$ [mm]	$\sigma(x^*)$ [μm]	$\sigma(\Theta_x^*)$ [μrad]
0.5	1.5	18	-3.9	-3.8	-0.080	1.26	6.0	16.6	30
2	0.49	18	-3.5	-4.0	-0.086	1.6	3.7	32	16
90	0	262	-1.9	0.0	-0.041	4.5	6.8	212	2.3
1535	100	270	0	0	-0.05	0.8	1.3	450	0.3

Table 1: Optics parameters at IP5 and at the RP220 station for the TOTEM running scenarios. L_x, L_y, v_x, v_y and D_x are the parameters of Equation 1 at RP220, $x_{\rm RP}$ and $y_{\rm RP}$ are the distances of the horizontal and vertical Roman Pots of the RP220 station from the beam centre, respectively, $\sigma(x^*)$ is the beam size at IP5 and $\sigma(\Theta_x^*)$ is the beam divergence at IP5.

low-β^* running scenarios. For $\beta^* = 1535\,\mathrm{m}$, the parallel-to-point focussing is achieved in both projections whereas for $\beta^* = 90\,\mathrm{m}$ only in the vertical one. In both cases, the large L_y pushes the protons vertically into the acceptance of the RP detectors.

Both optics also offer the possibility of detecting diffractive protons almost independent of their momentum loss. To be able to measure the momentum loss ξ with an acceptable resolution, L_x has to vanish to eliminate the dependence on the horizontal scattering angle Θ_x^* (cf. Equation (1)). This condition can only be achieved with the $\beta^* = 90\,\mathrm{m}$ optics (Table 1).

4 TOTEM Running Scenarios

The versatile physics programme of TOTEM requires different running scenarios that have to be adapted to the LHC commissioning and operation in the first years. A flexible trigger can be provided by the T1 and T2 telescopes and the Roman Pot detectors. TOTEM will take data under all optics conditions, adjusting the trigger schemes to the luminosity. The DAQ will allow trigger rates up to a few kHz without involving a higher level trigger. The high-β^* runs (Table 2) with 156 bunches, zero degree crossing-angle and maximum luminosity between 10^{29} and $10^{30}\,\mathrm{cm}^{-2}\mathrm{s}^{-1}$, will concentrate on low-$|t|$ elastic scattering, total cross-section, minimum bias physics and soft diffraction. A large fraction of forward protons will be detected even at the lowest ξ values. Low-β^* runs (Table 2) with more bunches and higher luminosity (10^{32} – $10^{34}\,\mathrm{cm}^{-2}\mathrm{s}^{-1}$) will be used for large-$|t|$ elastic scattering and diffractive studies with $-\xi > 0.02$. Hard diffractive events come within reach. In addition, early low β^* runs will provide first opportunities for measurements of soft diffraction at LHC energies and for studies of forward charged multiplicity.

5 Diffractive Proton Acceptance and Resolution

The acceptance and the reconstruction resolution are defined by the optics parameters via Equation 1. In addition, the beam divergence limits the $\Theta_{x,y}^*$-reconstruction resolution and thus

β^* [m]	k	$N/10^{11}$	$\mathcal{L}$ [cm^{-2}s^{-1}]	$\lvert t\rvert$-range [GeV^2] @ $\xi = 0$	ξ-range
1540	43 – 156	0.6 – 1.15	$10^{28} - 2 \cdot 10^{29}$	0.002 – 1.5	< 0.2
90	156	0.1 – 1.15	$2 \cdot 10^{28} - 3 \cdot 10^{30}$	0.03 – 10	< 0.2
11	43 – 2808	0.1 – 1.15	$\sim 10^{30} - 5 \cdot 10^{32}$	0.6 – 8	0.02 – 0.2
0.5 – 3	43 – 2808	0.1 – 1.15	$\sim 10^{30} - 10^{34}$	2 – 10	0.02 – 0.2

Table 2: Running scenarios at different LHC optics (k is a number of bunches, N — number of particles per bunch, and $\mathcal{L}$ — estimated luminosity). The $|t|$ ranges for elastically scattered protons correspond to the $\geq 50\%$ combined RP147 and RP220 acceptance.

the t-resolution, while the beam energy uncertainty $\sigma(p)/p$ limits the precision of longitudinal momentum loss reconstruction.

The acceptance and resolution of diffractive protons reconstructed with the Roman Pot devices, located at 220 m from IP5, are summarised in Tables 3–5.

In case of the low-β^* optics (Table 3), which is characterised by short effective length

β^* [m]	variable	acceptance	resolution
2	$\xi = \Delta p/p$	$0.02 < -\xi < 0.25$	$\sigma(\xi) \approx (1 - 6) \times 10^{-3}$
	DPE M [GeV]	$250 < M < 3000$	$\sigma(M)/M = 1 - 5\%$
	t [GeV^2]	complete t-range for $-\xi > 0.02$	$\sigma(t) \approx 0.3\sqrt{t}$
		$2 < -t_y < 10\,\text{GeV}^2$ @ $\xi = 0$	
	ϕ [rad]	$0 \leq \phi < 2\pi$	$0.15 < \sigma(\phi) < 0.5$ for $1 > -t > 0.05$ GeV^2

Table 3: Roman Pot acceptance and reconstruction summary for β^*=2 m optics at $\sqrt{s} = 14$ TeV.

(see Table 1), the protons are primarily accepted in the Roman Pots due to their fractional momentum loss ξ, independently of t. Because of the machine dispersion, they are shifted towards the horizontal Roman Pot. In this way all the t-range is accepted for $-\xi > 0.02$, as is demonstrated in Figure 2, left. The figure presents one of the early running scenarios characterised by reduced beam energy to 5 TeV.

On the contrary, in case of high-β^* optics (Tables 4 and 5), the protons are detected because of their four momentum transfer squared t, since the effective lengths are high (except L_x for $\beta^* = 90$ m). This results in full ξ-range acceptance for $-t > 0.02$ GeV and $-t > 0.003$ GeV for $\beta^* = 90$ m and 1535 m, respectively, as is illustrated by Figure 2, right. On average $\sim 50\,\%$ and $\sim 90\,\%$ of diffractive protons are accepted by RP detectors for $\beta^* = 90$ m and 1535 m, respectively.

The high-β^* scenarios, due to high effective lengths and low beam angular divergence, are characterised by good t- and ϕ-reconstruction capabilities and by acceptance of low $|t|$ values. The resolution in t changes depending upon the proton azimuth angle ϕ, its fractional momentum loss ξ (machine chromaticity) and the azimuth angle of proton. In case of $\beta^* = 1535$ m optics, for horizontal protons $\sigma(t_x) = (0.04 - 0.4)\sqrt{-t_x}$ while for vertical ones $\sigma(t_y) = (0.002 - 0.02)\sqrt{-t_y}$. The t-reconstruction precision in horizontal direction is generally lower

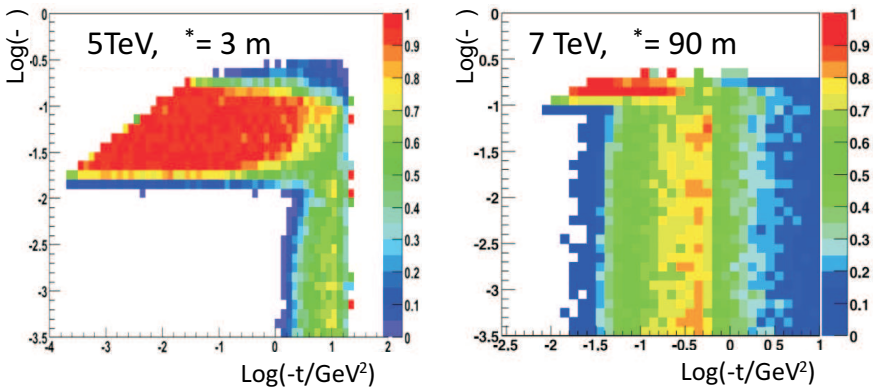

Figure 2: Acceptance in t and ξ of diffractively scattered protons at the RP220 station for the $\beta^* = 3\,\text{m}$ optics at $\sqrt{s} = 10\,\text{TeV}$ (left) and for the $\beta^* = 90\,\text{m}$ optics at $\sqrt{s} = 14\,\text{TeV}$ (right).

β^* [m]	variable	acceptance	resolution
90	$\xi = \Delta p/p$	complete ξ-range	$\sigma(\xi) \approx 0.006$ $\sigma(\xi) \approx 0.0015$ (CMS vtx.)
	DPE M [GeV]	complete M-range	$\sigma(M)/M < 1/2$ for $M > 150$
			$\sigma(M)/M < 1/2$ for $M \gtrsim 40$ (CMS vtx.)
	t [GeV^2]	$0.02 < -t < 10\,\text{GeV}^2$	$\sigma(t_x) \approx (0.3 - 0.4)\sqrt{-t_x}$ $\sigma(t_y) \approx 0.04\sqrt{-t_y}$
	ϕ [rad]	$0 \le \phi < 2\pi$	$0.02 < \sigma(\phi) < 1$ for $1 > -t > 0.01$ GeV^2

Table 4: Roman Pot acceptance and reconstruction summary for $\beta^* = 90\,\text{m}$ optics at $\sqrt{s} = 14\,\text{TeV}$. 'CMS vtx.' denotes the reconstruction scenario when primary vertex position, reconstructed in the CMS Tracker, is used in TOTEM proton reconstruction.

β^* [m]	variable	acceptance	resolution
1535	$\xi = \Delta p/p$	complete ξ-range	$\sigma(\xi) \approx 0.01$ (RP220)
			$0.002 < \sigma(\xi) < 0.006$ (RP220 + RP150)
	DPE M [GeV]	complete M-range	$0.05 < \sigma(M)/M < 0.6$ for $M > 300\,\text{GeV}$
	t [GeV^2]	$0.003 < -t < 1.5$	$\sigma(t_x) \approx (0.04 - 0.4)\sqrt{-t_x}$ $\sigma(t_y) \approx (0.002 - 0.02)\sqrt{-t_y}$
	ϕ [rad]	$0 \le \phi < 2\pi$	$0.002 < \sigma(\phi) < 0.02$ for $-t = 1$ GeV^2; $0.01 < \sigma(\phi) < 0.1$ for $-t = 0.05$ GeV^2;

Table 5: Roman Pot acceptance and reconstruction summary for β^*=1535 m optics at $\sqrt{s} = 14\,\text{TeV}$.

than in the vertical one because of shorter effective horizontal lengths and due to the fact that both the horizontal component of the scattering angle and the momentum loss displace the proton in the horizontal direction. As a result, the reconstruction of the horizontal scattering angle and of the momentum loss both depend upon the horizontal displacement, which limits

the resolution. The reconstruction of the azimuth angle ϕ is possible for all accepted t-values, however its resolution greatly improves for higher four momentum transfers.

In case of the low-β^* optics, the t-reconstruction is primarily limited by the beam divergence and is practically independent from the azimuth angle ϕ. The ϕ-reconstruction is possible only for $-t > 0.18$ GeV^2 and $-t > 0.05$ GeV^2, for $\beta^* = 0.5$ m and $\beta^* = 2$ m, respectively.

The cases of $\beta^* = 0.5$, 2 and 90 m are characterised by good ξ resolution of $\sigma(\xi) = 0.001$ – 0.006.

6 TOTEM Early Measurements

TOTEM will be operable from the LHC start and plans to profit from the early LHC beams. The first collisions are planned at the injection energy $\sqrt{s} = 900$ GeV and $\beta^* = 11$ m. For this scenario, due to large beam sizes and aperture limits, TOTEM RP acceptance is very limited [7]. Therefore, this scenario will be primarily used for experiment commissioning, alignment and calibration.

However, the LHC collisions planned at reduced beam energy of a few TeV and low-β^* [8] will allow for detection of SD and DPE events in T1, T2 and RP detectors (see Figure 1). In addition to the commissioning and alignment activities, TOTEM will conduct the preliminary measurements of the differential SD and DPE cross-sections $\mathrm{d}\sigma_{\mathrm{SD,DPE}}/\mathrm{d}M$ in the mass range of $1.4 < M < 4.2$ TeV and $0.2 < M < 1.8$ TeV, respectively, with mass reconstruction precision $\sigma(M)/M = 2$–$4\,\%$. In addition, T1 and T2 telecsopes will study the topology of diffractive events. In particular, they will make an attempt to measure the rapidity gaps $\Delta\eta$ of diffractive systems which can be further compared to the reconstructed proton momentum loss $\xi = \Delta p/p$ via the relation $\Delta\eta \approx -\ln|\xi|$. Also the pp elastic scattering differential cross-section $\mathrm{d}\sigma/\mathrm{d}t$ for $2 < -t < 10$ GeV will be measured in this scenario with a precision $\sigma(t)/t \approx 0.3\sqrt{|t|}$.

TOTEM will also contribute to the multiplicity studies of forward particles, which are essential not only for minimum bias MC simulations but also for cosmic rays' physics. The energy and mass of ultra-high-energy cosmic rays are obtained with the help of Monte Carlo codes which describe the shower development (dominated by forward and soft QCD interactions) in the upper atmosphere. Various high-energy hadronic interaction models differ of factors up to three, with significant inconsistencies in the forward region ($|\eta| < 5$). The measurements of forward events' topology, carried out by T1 and T2 telescopes, should help to tune the MC codes.

7 Later Diffractive Studies

Due to large rapidity coverage of T1 and T2 detectors ($3.1 \leq |\eta| \leq 6.5$), TOTEM alone can study diffraction extensively by means of rapidity gaps and forward proton detection. In addition, the physics programme can be further extended by cooperation between TOTEM and CMS, which will provide the largest acceptance detector ever built at a hadron collider [3]. This will create a unique opportunity to measure the rapidity gaps in the range of $|\eta| < 6.5$ together with efficient proton reconstruction. In addition, the trigger, based on forward protons, on central system topology and multiplicity, and on calorimetry information, will provide clean signatures for specific processes and efficient background rejection. This will allow for a versatile diffractive physics programme which will cover soft-diffraction, studied at high-β^* optics and low luminosity runs (see Table 2), semi-hard and hard diffractive processes, such as jet-jet

production, characterised by low cross-sections, which require higher luminosities and thus low-β^* optics [3].

The CMS TOTEM cooperation not only extends the available acceptance but it also improves the reconstruction. In particular, the CMS Tracker can provide the primary vertex position with a resolution of $\sim 30\,\mu$m, which highly reduces the uncertainty of longitudinal proton momentum reconstruction for the $\beta^* = 90\,$m case, as can be seen in Table 4. The calorimetry system of CMS, in addition to a $\mathbf{p}_T$-trigger, yields an additional means of diffractive system mass determination [9, 10] based on measurement of transverse energy E_{T_i} of centrally produced objects at rapidities η_i: $\xi_{1,2} = \sum_i E_T^i \mathrm{e}^{-\eta_i}/\sqrt{s}$. The prospects for diffractive physics are discussed in detail in [3].

8 Conclusions

The TOTEM physics program aims at deeper understanding of proton structure by measuring the total and elastic *pp* cross sections and by studying a comprehensive menu of diffractive processes. TOTEM will run under all LHC beam conditions to maximise the coverage of the studied processes. Special high-β^* runs are needed for the total *pp* cross section measurement with the luminosity-independent method and for soft-diffraction with large forward proton acceptances. Early low-β^* runs will provide first opportunities for measurements of soft diffraction in central and single diffractive events, as well as studies of the forward charged multiplicity in inelastic *pp* events. Finally, hard diffraction as well as many forward physics subjects will be studied in collaboration with CMS taking advantage of the unprecedented rapidity coverage for charged and neutral particles.

References

[1] The TOTEM Collaboration, *Technical Design Report*, CERN-LHCC-2004-002; addendum CERN-LHCC-2004-020.

[2] The TOTEM Collaboration, *The TOTEM Experiment at the LHC*, 2008 JINST 3 S08007, doi: 10.1088/1748-0221/3/08/S08007.

[3] The CMS and TOTEM diffractive and forward working group, *Prospects for Diffractive and Forward Physics at the LHC*, CERN/LHCC 2006-039/G-124, 2006.

[4] E. Wilson, *An Introduction to Particle Accelerators*, Oxford University Press, 2006.

[5] H. Niewiadomski, *Reconstruction of Protons in the TOTEM Roman Pot Detectors at the LHC*, PhD dissertation, Manchester, 2008.

[6] V. Barone, E. Predazzi, *High-Energy Particle Diffraction*, Springer 2002.

[7] H. Niewiadomski, *Acceptance of Protons in the TOTEM RP Detectors for LHC V6.500 Optics of Injection Energy ($E = 450\,$GeV, $\beta^* = 11\,$m)*, TOTEM-NOTE-2009-001, 2009.

[8] H. Niewiadomski, *Acceptance of Protons in the TOTEM RP Detectors for LHC V6.500 Early Collision Optics ($E = 5\,$TeV, $\beta^* = 3\,$m)*, TOTEM-NOTE-2009-002, 2009.

[9] D. Acosta et al., CDF Collaboration, Phys. Rev. Lett. 93 (2004) 141601.

[10] V. M. Abazov et al., D0 Collaboration, *Hard single diffraction in $p\overline{p}$ collisions at $\sqrt{s} = 630\,$GeV and 1800 GeV*, Phys. Lett. B531 (2002) 52.